APPLICABILITY OF FLAT PLATE METHODS IN DETERMINING FLUID/STRUCTURE INTERACTION EFFECTS IN BWR PRESSURE SUPPRESSION SYSTEMS

G. S. HOLMAN, E. W. McCAULEY, S. C. H. LU
University of California, Lawrence Livermore Laboratory,
P.O. Box 808, Livermore, California 94550, U.S.A.

Abstract

Flat plate chord tests are one experimental method used to investigate how fluid/structure interaction (FSI) effects modify the impulsive loading in nuclear reactor pressure suppression pools. This analytical study examines the applicability of using a flexible flat plate in an otherwise rigid shell to model dynamic pool wall response in a flexible shell pressure suppression torus. Bubble pressures varying by a factor of seven are used as input to two-dimensional finite-element models. Boundary response to various plate and shell thicknesses are compared on the basis of equivalent natural frequency. Results indicate the qualitative flat plate response compares well with the flexible shell but absolute pressures vary significantly and nonconservatively.

This work was supported by the U.S. Nuclear Regulatory Commission under Interagency Agreement DOE 40-550-75 with the U.S. Department of Energy.

1. Introduction

The General Electric Mark I boiling water reactor (BWR) pressure suppression system (Figure 1) consists of a light-bulb shaped concrete caisson (the "drywell") connected by large pipes to a toriodal steel shell (the "wetwell") partially filled with water. In the case of a hypothetical loss-of-coolant accident (LOCA), high-pressure steam venting from a pipe break within the drywell is injected into the suppression pool where it condenses, maintaining the overpressure of the concrete containment within acceptable structural limits. The pool also serves as a thermal sink for steam periodically discharged from the reactor vessel safety relief valves as a part of normal BWR operation. In either case, the discharge of steam into the pool, together with noncondensible air that is forced ahead of the steam, induces hydrodynamic loads on the suppression torus. Since the suppression torus acts as the primary BWR safety system, a thorough understanding of the hydrodynamic loading of the torus shell is necessary to assure containment integrity under all conditions.

Most analytical and experimental approaches to this problem treat the shell as rigid when, in fact, the shell in real systems is flexible. The qualitative effect of shell flexibility on hydrodynamic loading in the suppression pool was the subject of an analytic research program conducted by the Lawrence Livermore Laboratory for the U.S. Nuclear Regulatory Commission (NRC)[1,2]. Part of this program included two-dimensional linear finite-element analyses of hydrodynamic loads induced by a nominal safety relief valve (SRV) air discharge and a nominal LOCA air discharge. These analyses modeled an idealized planar cross section of the torus and indicated that attenuation of hydrodynamic loads is enhanced by increasing wall flexibility.

The analytic study described here models a SRV discharge pulse to examine the applicability of using a flexible flat plate in an otherwise rigid shell to model dynamic pool wall response in a flexible shell pressure suppression torus. Flat plate chord tests are one experimental method often used to investigate how fluid/structure interaction (FSI) effects modify impulsive loading in such systems and offer an economical means of varying flexibility over a wide range. A theoretical equivalence between a flexible shell of a given thickness and a flexible plate of a given (but not necessarily equal) thickness can be arrived at on the basis of equivalent natural frequency, but other questions regarding equivalence of behavior arise, namely how the physical presence of the plate affects the pressure distribution in the pool and how the actual peak pressure attenuation predicted using the plate compares both qualitatively and quantitatively with that predicted by the flexible-shell analyses.

2. Analytic Models

The two-dimensional idealization of the torus for the flexible-shell analyses (Figure 2) represents a right circular cylinder 421.7 cm in radius filled with water to a level 91.44 cm below that of the shell horizontal centerline. Shell flexibility is characterized by the ratio of the minor diameter of the torus (D) to the thickness of the shell (t), with a D/t ratio of zero denoting absolute rigidity. The primary dimensions of the model are taken from the Monticello power plant operated by the Northern States Power Company of Minnesota. The Monticello torus D/t ratio is approximately 580, a value representative of the Mark I containment system.

The "ram's head" SRV discharge header used in the actual system is modeled by a single bubble 25.4 cm in diameter located 279.4 cm below the elevation of the shell horizontal centerline. The bubble inner surface is loaded by 60 ms of a nominal SRV pressure pulse (Figure 3), divided into 0.5 ms finite time steps. This theoretical pulse is derived from Rayleigh bubble arguments and has a peak overpressure of 1.035 MPa (10.35 bars).

The two-dimensional flexible-shell model uses 634 nodal points to form the finite-element mesh (Figure 4). A total of 545 four-node quadrilateral fluid elements is used, 520 of which have the bulk material properties of water with a trace shear modulus (approximately six orders of magnitude less than the bulk modulus) included to stabilize the nearly incompressible problem. The slip condition along the shell interface is simulated by 25 "zero shear" fluid elements which retain the bulk properties of water, but have no shear capacity at all. The steel shell is modeled by 29 quadrilateral thin-shell elements with material properties typical for structural steel.

The model is rigidly constrained at the upper edge with the usual displacement and rotational symmetry constraints applied along the shell vertical centerline.

To model the flexible plate in a rigid shell, a flat plate is introduced into the flexible-shell model with its center 30 deg relative to the shell vertical centerline (Figure 5). The plate subtends an arc of 40 deg and is pinned at its lower end (10 deg) and roller-mounted at its upper end (50 deg). This particular configuration was arbitrarily based on a similar configuration used in an actual (although much smaller scale) experiment. The finite-element mesh (Figure 6) has 714 nodal points and a total of 571 fluid elements. The mesh density in the body of the fluid is the same as for the flexible-shell model (520 elements), the additional elements being required to define the slip condition along both the plate and the shell interfaces. Material properties are identical to those used in the flexible-shell model.

As with the flexible-shell model, the usual symmetry constraints are applied to the flexible-plate model. Shell rigidity in this case is defined by constraining each of the shell nodes absolutely. The same nominal SRV pressure pulse is used to load the inner surface of the bubble.

3. Two-Dimensional Analyses

Analyses of both the flexible-shell and flexible-plate models were conducted using DTVIS2, a two-dimensional plane or axisymmetric implicit finite-element computer code. A detailed description of DTVIS2 is included in Ref. [2].

Time histories of pool pressure calculated at the pool bottom for flexible-shell D/t ratios of 0, 300, and 600 are shown in Figure 7, normalized to the peak source pressure. In general, the pressure response exhibits a well-defined peak with late oscillations about a carrier which follows the basic shape of the input pulse. The peak pressure decreases as shell flexibility increases, while the response pulse is broadened and shifted in time as shell flexibility increases. The general conclusion drawn from the results of these analyses is that torus wall flexibility will decrease the peak pressures seen by the shell wall. It is therefore implied that analytical or experimental results obtained for rigid or nearly rigid systems will be conservative when applied to the design of highly flexible real systems.

A companion series of flexible-plate analyses was run for plate thicknesses corresponding to shell-diameter-to-plate-thickness ratios of 0, 300, and 600. When compared to similar shell-diameter-to-shell-thickness ratios on the basis of natural frequency, these values translate to equivalent shell D/t ratios of 0, 246, and 492 respectively.

A comparison between rigid models with and without the internal plate was first made to determine the possible effect of inserting the flat plate into the finite-element model. A comparison of pressure response at the pool bottom (Figure 8) and pressure contours in the pool at the time of peak input pressure (Figure 9) indicates that the pressure response in the rigid system is essentially unperturbed by the presence of the plate per se. However, when the pressure response at the plate center is compared to that at the pool bottom (Figure 10), it can be seen that while the character of the pressure response at each location is quite similar, the magnitude of the peak pressure at the plate center is significantly less than at the pool bottom. In general, the peak pressure measured along the plate decreases compared with that at the pool bottom with increasing distance from the pool bottom (Figure 11). This same effect is observed when flexible plates inside of the rigid shell are considered (Figure 12).

A summary of peak pressure as a function of equivalent shell D/t ratio (Figure 13) shows how both analytic models indicate enhanced attenuation of the input pressure pulse as plate or shell flexibility increases. However, when peak pressures at the plate center are compared to those at the pool bottom for the corresponding flexible shell (no internal plate), the plate pressure is as much as a factor of three lower. As stated previously, this factor may further increase if plate pressures calculated away from the plate center are considered.

A companion set of flexible-plate analyses was also performed for a geometrically similar problem under different loading conditions. For these analyses, the bubble was positioned along the shell vertical centerline at the same elevation as the ends of the downcomers, then was loaded with a theoretical LOCA chug air discharge pulse. This new input condition is represented by a 80 ms single sawtooth pulse with a peak pressure of 0.138 MPa (1.38 bars). Despite the less impulsive nature of the LOCA input pulse, a comparison of pressure response predicted at the plate center with that predicted by the SRV flexible-plate model (Figure 14) shows essentially the same behavior.

4. Conclusions

It is recognized that weaknesses in the two-dimensional representation of the Mark I pressure suppression torus limit the ability of this simple model to actually quantify the magnitude of the hydrodynamic attenuation that results from shell wall flexibility. In particular, the two-dimensional "bubble" in the model actually represents a cylindrical source of infinite extent, therefore implying an unrealistically large energy input to the problem. Furthermore, the two-dimensional shell does not treat the additional degrees of flexibility that are present in the actual three-dimensional system. It is useful to note, however, that a series of three-dimensional finite-element analyses of one torus bay[2] under the same nominal SRV loading, using a true spherical source to represent the bubble, produced the same qualitative behavior predicted by the two-dimensional model (i.e., that hydrodynamic loads are attenuated by increasing shell flexibility), but indi-

cated significant reductions in the peak magnitudes of the pressures predicted.

Such weaknesses in the two-dimensional model do not, however, necessarily invalidate the qualitative conclusions that can be drawn from the results of the flexible-shell vs. flexible-plate comparison. Within the recognized limitations of the two-dimensional modeling, the results of the study indicate that the flat plate captures the general character of the pressure response of the flexible shell and indicates the same qualitative dependence of hydrodynamic loading on wall flexibility. However, the lower absolute pressures predicted by the flexible-plate model imply non-conservative pressure attenuation due to flexibility. The results of this study indicate, therefore, that caution should be exercised in the application of flat plate experimental data for the evaluation of flexible shell behavior.

References

[1] MC CAULEY, E. W., and MARTIN, R. W., "Effect of Torus Wall Flexibility on Forces in the Mark I BWR Pressure Suppression System", Lawrence Livermore Laboratory, Livermore, California, Report UCRL-52506, June 1978.

[2] LU, S. C., HOLMAN, G. S., and MC CAULEY, E. W., "Effect of Torus Wall Flexibility on Forces in the Mark I BWR Pressure Suppression System", Lawrence Livermore Laboratory, Livermore, California, Report UCRL-52624, December 1978.

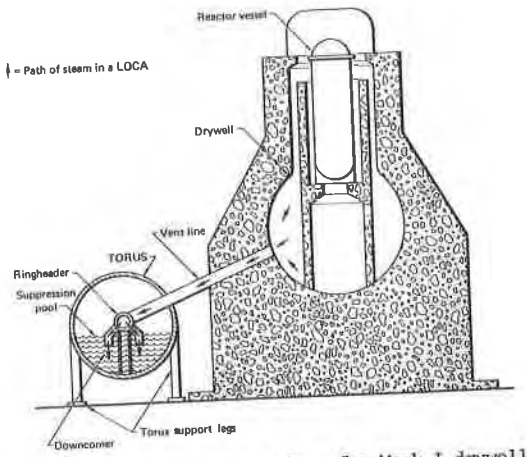

1. Schematic representation of a Mark I drywell and torus, showing the steam flow path during a loss-of-coolant accident (LOCA).

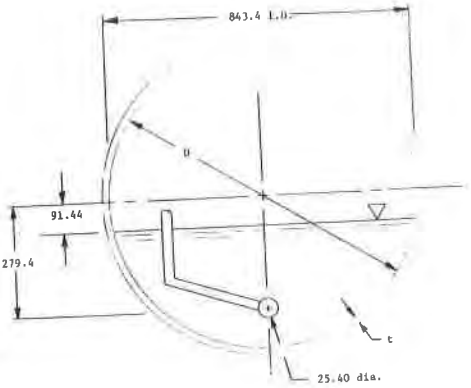

Note: all dimensions in cm

2. Two-dimensional representation of SRV torus with reference dimensions.

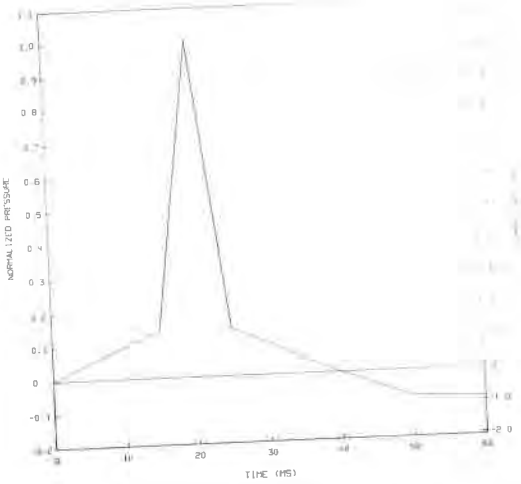

3. Nominal SRV pressure input pulse.

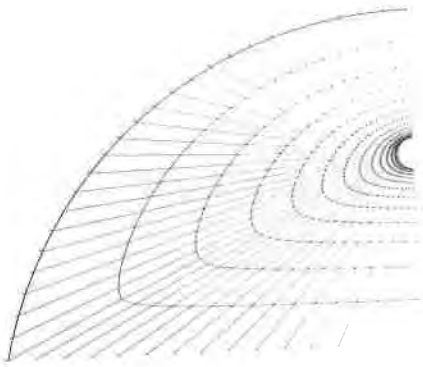

4. Two-dimensional finite-element mesh for flexible-shell model.

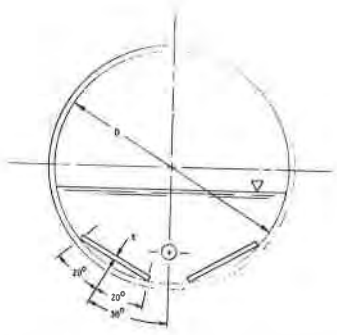

5. Two-dimensional representation of SRV torus with internal plate.

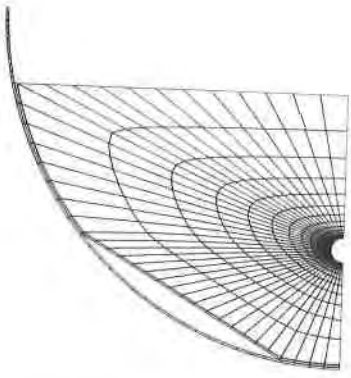

6. Two-dimensional finite-element mesh for flexible-plate model.

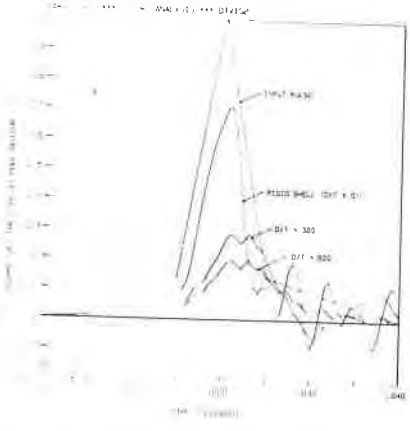

7. Pressure response at pool bottom calculated using flexible-shell model.

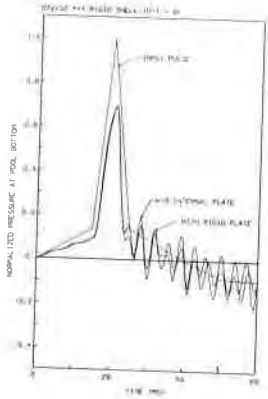

8. Comparison of pressure response at pool bottom calculated for rigid shells with and without rigid internal plate.

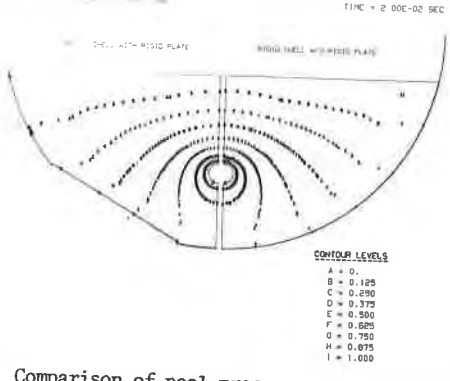

9. Comparison of pool pressure contours calculated at 20 ms for rigid shells with and wit rigid internal plate.

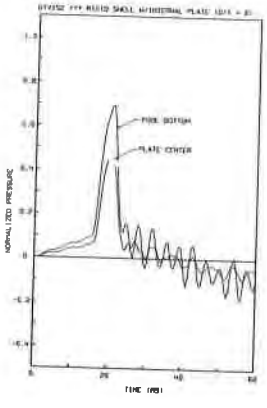

10. Comparison of pressure response at pool bottom and at center of rigid internal plate.

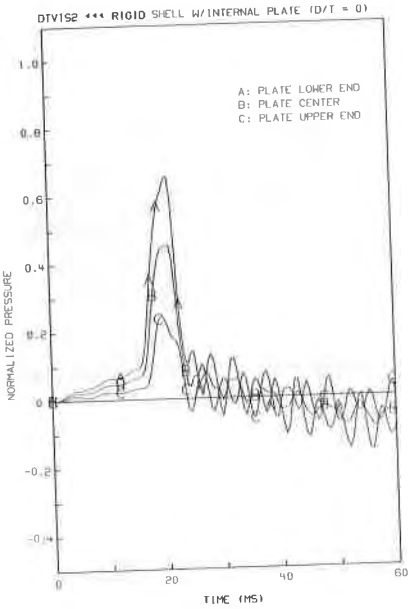

11. Comparison of pressure response calculated at indicated locations along the rigid internal plate.

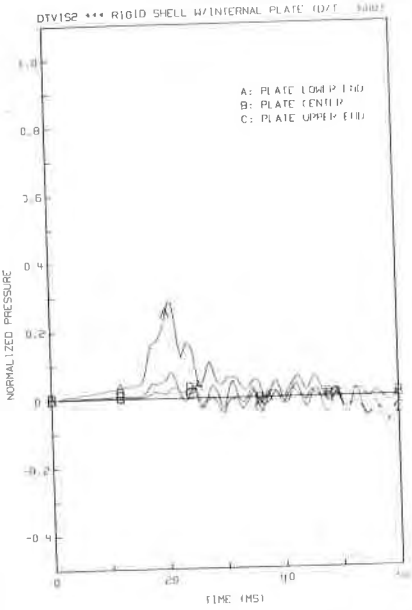

12. Comparison of pressure response calculated at indicated locations along the flexible internal plate (plate D/t = 600).

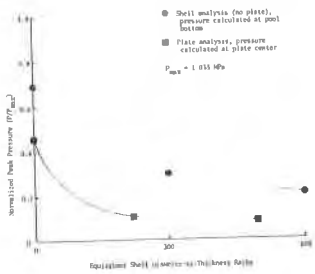

13. Comparison of peak pressure vs. D/t ratio calculated by flexible-shell and by flexible-plate analyses.

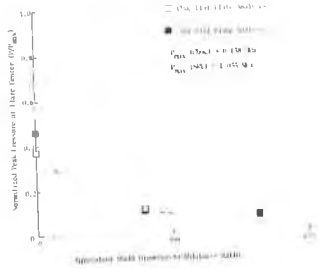

14. Comparison of peak pressures calculated by flexible-plate analyses using nominal SRV and LOCA chug input pulses.